AIAA 95-3848

The Applications of Smart Structures for Vibration Suppression in Spacecraft

William B. Harrington, Jr. and Brij N. Agrawal
Naval Postgraduate School
Monterey, CA

AIAA 1995 Space Programs and Technologies Conference
September 26-28, 1995/Huntsville, AL

THE APPLICATIONS OF SMART STRUCTURES FOR VIBRATION SUPPRESSION IN SPACECRAFT

William B. Harrington, Jr.*
Brij N. Agrawal**
Naval Postgraduate School
Monterey, CA, USA

Abstract

This paper presents the smart structures technology program at the Naval Postgraduate School. The research program consists of vibration damping of space structures using piezoceramic sensors and actuators, vibration isolation of space structures using H_∞ wave absorbing control, and the development of parameter optimization techniques to minimize antenna pointing errors. Several new control laws are experimentally implemented using an air-bearing flexible spacecraft simulator (FSS) representing a spacecraft with smart structures. The major emphasis has been to improve performance of flexible spacecraft antenna using the latest smart structure technology. Both analytical and experimental research is performed in the Spacecraft Controls Laboratory.

I. Introduction

Several future civilian and military spacecraft will require active damping for large flexible structures, vibration isolation of optical payloads, and shape control of reflector and optical benches to meet performance requirements. For these type of applications, smart structures is a promising technology. In general, smart structures are the system elements that sense the dynamic state and change the system's structural properties, such as its natural frequencies and its damping, to meet given performance objectives.

There are several types of embedded sensors and actuators which can be used for vibration control. The embedded sensors are piezoelectric deformation sensors, strain gages, and fiber optic sensors.[1] The embedded actuators are piezoceramic wafers, electrostrictive ceramic wafers, piezoceramic polymer film and shape memory metal wires. For the research program at the Naval Postgraduate School, piezoceramic sensors and actuators are currently used, additionally a Vision Server camera system is used as an external optical sensor for the FSS. Piezoceramic sensors have a high strain sensitivity , a low noise baseline, low to moderate temperature sensitivity, and an ease of implementation. Piezoceramic actuators have high stiffness, sufficient stress to control vibration, good linearity, temperature insensitivity, are easy to implement, and minimize power consumption.

Initial motivation for research in smart structures was to provide active damping to the flexible structure of Flexible Space Simulator (FSS) shown in Figure 1. This discussion provides an overview of the research program on smart structures at the Naval Postgraduate School.

II. Research Program 1990 - 1995

The Flexible Spacecraft Simulator (FSS) simulates attitude motion about the pitch axis of a spacecraft. It consists of a single degree-of-freedom rigid central body, representing the spacecraft central body, and a multiple degree-of-freedom flexible appendage, representing an antenna reflector with a flexible support structure. Piezoceramic sensors and actuators are used to provide active damping to the flexible support structure. The entire system is floated on air pads over a finely ground granite

---

* Lieutenant Commander, United States Navy, Student Member AIAA
** Professor, Department of Aeronautics and Astronautics, Associate Fellow AIAA

table to simulate a microgravity environment. The central body has two thrusters and a momentum wheel as its actuators.

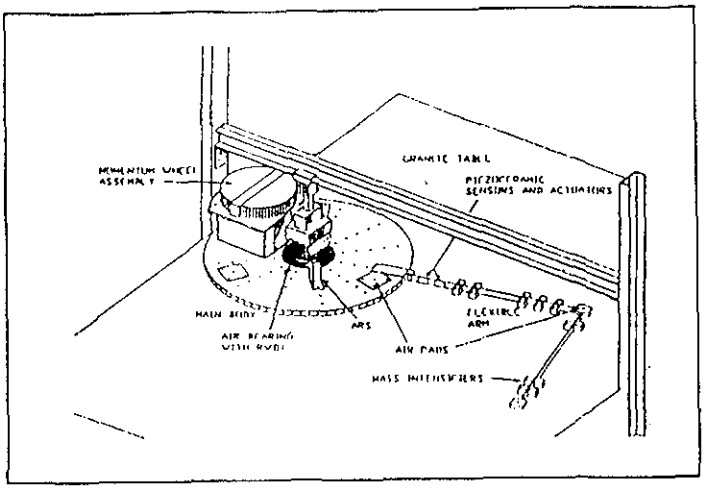

Figure 1. NPS Flexible Spacecraft Simulator (FSS)

Piezoceramic sensors and actuators are located on the flexible appendage as shown in Figure 2. The piezoceramic wafers are bonded to the surface of the flexible arm and the voltage developed from the sensors is fed to the actuators in such a way that motion of the flexible arm is damped. Figure 3 illustrates the orientation of a piezoceramic wafer on an arm and the alignment of its axis that describes the electro-mechanical relationships.[2]

The piezoceramic wafers in a sensory mode produce a charge between their electrodes that is directly proportional to the lateral strains. It is given by

$$Q = AEd_{31}(\varepsilon_1 + \varepsilon_2) \tag{1}$$

where A is the lateral area of the piezo wafers, E is Young's modulus of the wafer, d_{31} is the lateral charge coefficient, and ε_1 and ε_2 are the strain values in the lateral directions respectively. The capacitance for a piezoceramic wafer as shown in Figure 3 is given by

$$C = \frac{DA}{t} \tag{2}$$

where D is the dielectric constant of the piezoceramic and t is the thickness of the wafer.

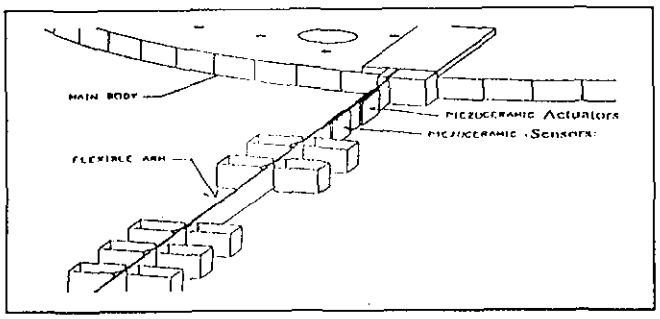

Figure 2. Sensor Actuator Placement for FSS Beam

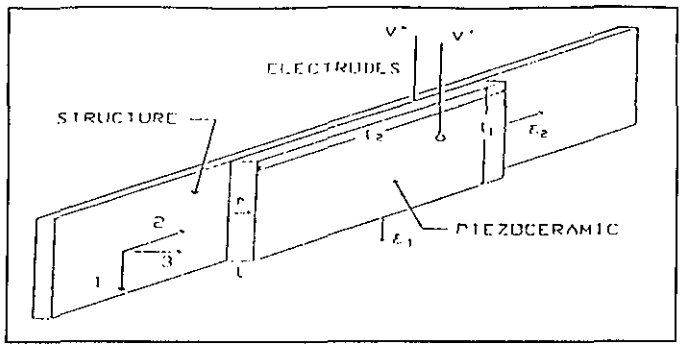

Figure 3. Piezoceramic Mounting on FSS Beam

The voltage V produced by a sensor under strain is given by

$$V = \frac{Q}{C} = \frac{Ed_{31}}{D} t(\varepsilon_1 + \varepsilon_2) \tag{3}$$

When using piezoceramic wafers as actuators, the attachment geometry is similar to the sensor geometry shown in Figure 3. The control voltage , e_c , is applied to the wafers and the lateral strain that is developed can act to control the bending of the beam. The electric field that is developed by the wafer is given by

$$\Phi = \frac{VC}{t} \tag{4}$$

Care must be taken not to induce a strong electric field that is opposed to the piezo's poling direction as that can damage the material by depolarizing it. Typical field limits by most materials are between 500 and 1000 volts/mm.

One of the first methods employed to damp the flexible appendage is positive position feedback (PPF). In order to implement this control law on the FSS, it is modeled as a second order system:

$$\begin{aligned} \ddot{\xi} + 2\zeta\omega\dot{\xi} + \omega^2\xi &= g\omega^2\eta \\ \ddot{e}_c + 2\zeta_c\omega_c\dot{e}_c + \omega_c{}^2 e_c &= -\omega_c{}^2 k e_s \end{aligned} \tag{5}$$

ξ is the modal coordinate of the structure

ω is the structural resonant frequency

ζ is the structural damping ratio

η is the modal coordinate of the compensator

e_c is the actuator applied voltage

e_s is the sensor sensed voltage

ζ_c is the actuator damping ratio

ω_c is the actuator frequency

k is the actuator gain

For this method of control initially an analog compensator was used. Figure 4 shows the damping with and without a PPF controller.

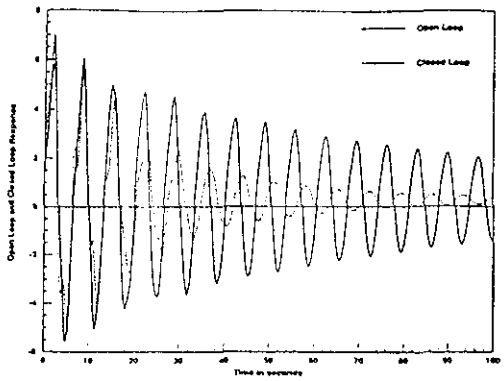

Figure 4. Positive Position Feedback Response

By setting the actuator frequency equal to the structure fundamental frequency, a 90° phase shift is attained in the region where $\omega_c / \omega_{n1} = 1$. ω_{n1} is the fundamental structural frequency. This equation is added into the system state-space representation as an additional two states. Figure 5 illustrates that the effect of this type of compensation is an active damping region in the area of $\omega_c / \omega_{n1} = 1$ with active stiffness for frequencies above this region and active flexibility in the frequencies below this region.

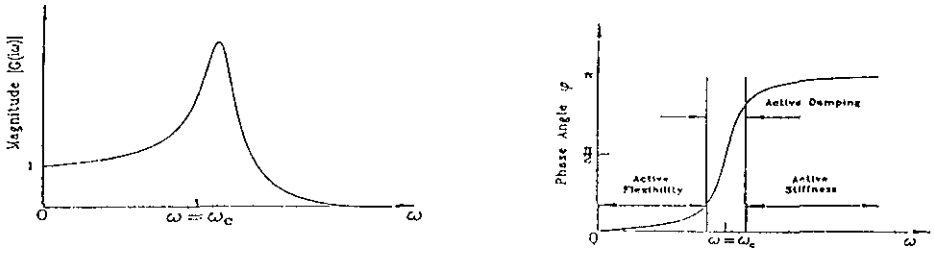

Figure 5. PPF Gain and Phase Plots

Thus it is important to set the actuator frequency at the fundamental structural frequency to avoid an increase in flexible mode strength for lower frequencies. This concept was verified in a study conducted to compare the control authority between single and multiple sensor/actuator systems.

An analysis was performed on a multi-modal vibration suppression system.[3] Specifically, the first three modes of a cantilevered beam were to be controlled using two different schemes. First, using three collocated sensors/actuators pairs connected to three compensators which were tuned to the beam's first three modal frequencies, and second, using a single collocated sensor/actuator pair connected to the three compensators. Figures 6a and 6b illustrate the block diagrams of these two control schemes.

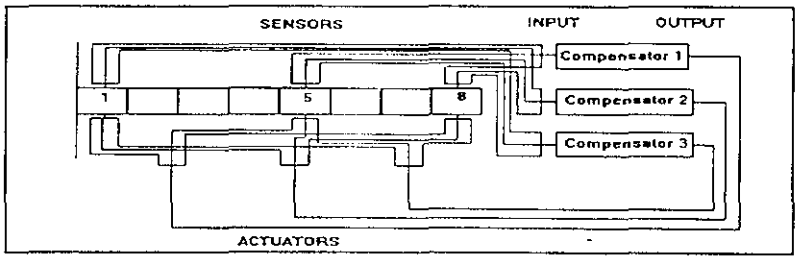

Figure 6a. Multi-Sensor/Actuator Arrangement

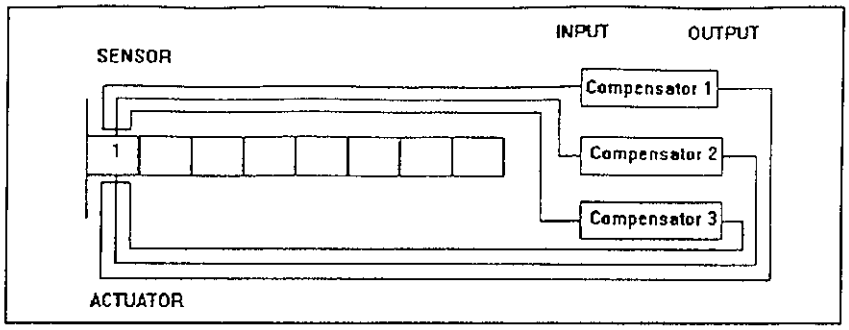

Figure 6b. Single Sensor/Actuator Arrangement

Figure 7 shows the response of the beam under the influence of three actuators, at the base, the middle, and at the tip of the beam. The effectiveness of this type of system is seen in how quickly all three modes are suppressed. Figure 8 indicates that, using the second system setup, a sufficient amount of control is obtained with the single actuator located at the root of the beam. The effect of actuator placement is evident when Figure 8 is compared with Figures 9 and 10 which show the beam's response with actuators located in the middle and at the tip of the beam, feeding their respective compensators with the same gains. However, their performance can be improved by increasing the gains. Individual modal responses can be tailored by varying the gains such that the damping of one mode is maximized in relation to the other modes.

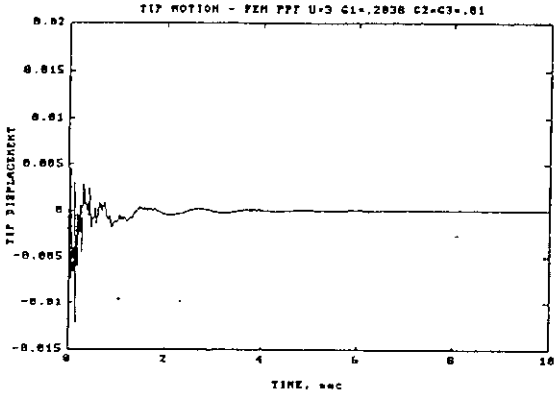

Figure 7. PPF Three Actuators Mode

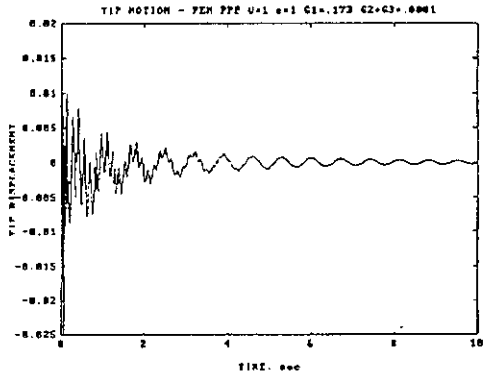

Figure 8. PPF Root Mounted Actuator

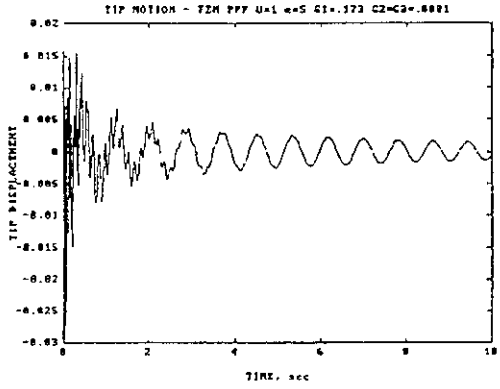

Figure 9. Middle Mounted Actuator

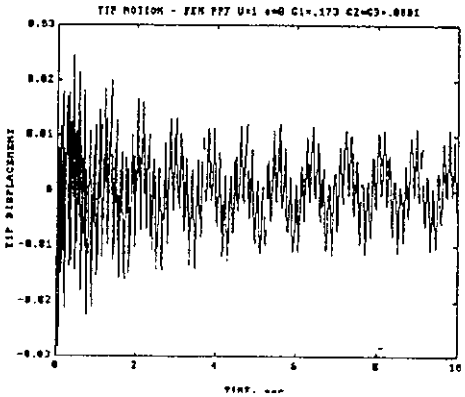

Figure 10. Tip Mounted Actuator

The next step was to integrate digital control into the spacecraft simulation system.[4] The FSS was connected to a Digital Equipment Corporation VAX 3100 computer system and the Integrated Systems, Inc. AC-100 real time control processor. Along with $Matrix_X$, the VAX computer system was used to compare digital performance of derivative control, integral control and positive position feedback control.

The procedure was to explore the performance of different control approaches using a digital controller and comparing the results to those obtained previously using "modified" PPF control. Open and closed loop runs were performed. Most of the runs attempted to excite the arm's fundamental mode without appreciably exciting the higher modes, however, many runs did have multiple mode excitation.

The primary performance indicator used for comparison between PPF and Phase Lead models was damping ratio, ζ. The damping ratio was calculated by the log decrement method:

$$\zeta = (\frac{1}{2\pi n}) \ln(\frac{A_i}{A_f}) \qquad (6)$$

where A_i is the initial amplitude, A_f is the final amplitude, and n is the number of cycles between the two amplitudes measured. The observed damping ratios were small enough to assume that the damped frequency was equal to the natural frequency.

The PPF controller was able to obtain a 187% increase in damping for the fundamental mode and a 167% increase in damping for the multimode response. The best PPF multimode response was obtained by damping only the first mode, attempts to control the second mode tended to degrade overall damping performance. Figures 11 and 12 are the beam responses for the PPF controller.

Phase lead controllers with sensor-actuator phase angles approaching 90° were first attempted. However, choosing controller gains low enough so as not to cause instability in the arm's response resulted in unacceptably low damping ratios. The instability is believed to be caused by the time delays in the controller circuitry and the associated phase shifts through the digital controller. At a phase angle of 88.88° a 42% increase in damping was achieved, and with the same phase angle, the multimode response resulted in a 32% increase in damping. The sensor-actuator phase relationship was then reduced to 60°. This allowed the use of higher controller gains while preserving the controller's ability to damp higher modes. Figures 13 and 14 show favorable performance. The fundamental mode response was a 72% increase in damping with a 100% increase in damping for the multimode response.

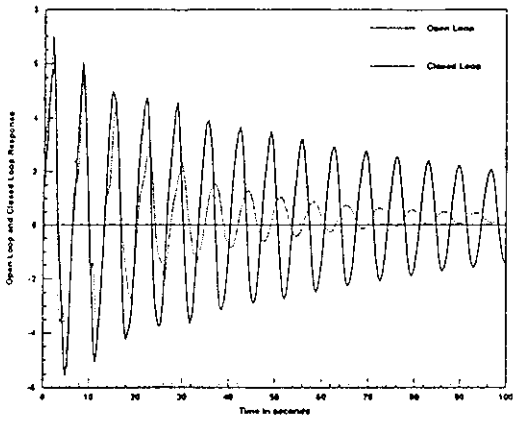

Figure 11. PPF Fundamental Mode

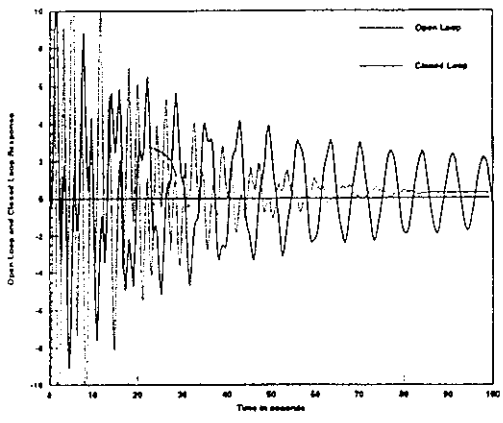

Figure 12. PPF Multimode

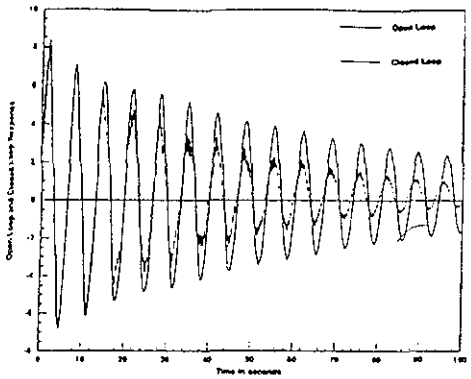

Figure 13. Phase Lead Fundamental Mode

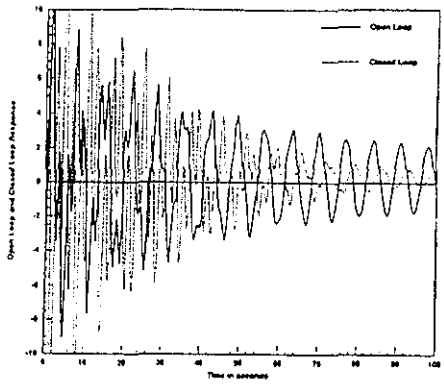

Figure 14. Phase Lead Multimode

The integral controller was originally studied with unsatisfactory results. Continuous activation of the controller was allowing integration of small system biases, resulting in degraded controller performance. A modified approach was taken whereby the actuator was not activated until immediately before it was required. Figures 15 and 16 show the favorable results. A 139% increase in damping was the fundamental mode response with a 100% increase in damping for the multimode response.

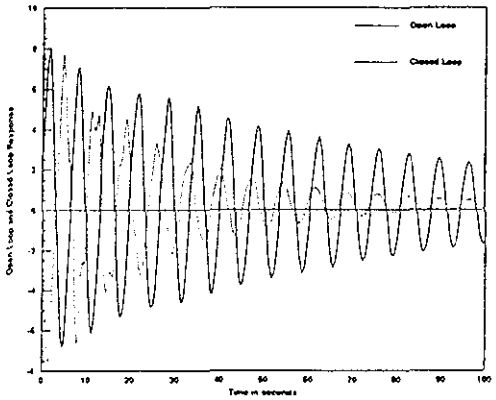

Figure 15. Integral Fundamental Mode

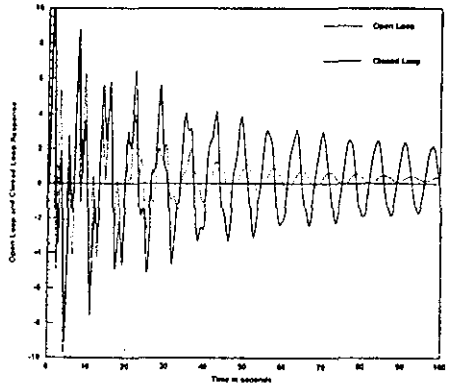

Figure 16. Integral Multimode

A summary of the comparison results, measured as damping ratios, ζ, is shown in Table 1.

Control Mode	Open Loop (1st/2nd Modes)	Closed Loop (First Mode)	Closed Loop (Higher Modes)
Modified PPF	0.0142/0.0183	0.0408	0.0489
Phase Lead (ϕ=90°)	0.0142/0.0183	0.0202	0.0241
Phase Lead (ϕ=60°)	0.0142/0.0183	0.0243	0.0367
Integral	0.0142/0.0183	0.034	0.0367

Table 1

A study was initiated to solve for optimal control gains for multiple-input multiple-output (MIMO) systems using PPF.[5] Stability criterion was established for the two, second order, system and compensator equations as:

$$\Omega - a_1 a_2 C^T G C > 0 \tag{7}$$

where Ω is the modal natural frequency matrix, a_1 and a_2 are constants representing actuator and sensor sensitivity respectively, C is the sensor state vector, and G is the feedback gain matrix. Notice the matrix should be positive definite and the stability criterion in Eq. (7) does not depend on the structural properties of the compensator.

Motivated by general optimization of a Linear Quadratic Regulator (LQR) cost function it is suggested to minimize the following cost function by the feedback gains being subject to the constraint equation, Eq. (7).

$$J(p) = \frac{1}{2}\int_0^\infty (x^T Q_s x + u^T Q_u u)dt \tag{8}$$

$p \equiv [p_1, p_2, \cdots, p_n]$ is a vector of design parameters consisting of feedback gains

$x = [\eta, \dot{\eta}, \xi, \dot{\xi}]^T$ is a state vector for the system in first order state space form

This approach was implemented on the FSS with the intent of minimizing the flexible arm tip deflection and rotation. An optimization algorithm using Homotopic Nonlinear programming was successfully applied to designing an optimized PPF compensator for control of the flexible spacecraft model using adaptive structures. The results verify that the proposed method can be used to improve the performance over the conventional PPF approach.

Recently, the effects of H_∞ optimized wave absorbing control were studied on the FSS with a cantilevered beam.[6] A major advantage of this method is that it does not involve truncation into a finite dimensional mathematical model. A closed loop scattering matrix was derived which gives the relationship between incoming waves, outgoing waves, sensor, and actuator. The control law was determined by minimizing the H_∞ norm of this matrix. The H_∞ wave absorbing controller contributed significant damping to the structure, especially at its fundamental mode of 1 Hz.

This approach describes the structural response of the system in terms of an elastic disturbance which travels through the structure.[7] In this approach compensators were designed to reduce the effects of incoming waves on outgoing waves. The advantages of the wave absorbing control are: relative ease of implementation, broad-band control, and no requirement for a finite element or modal model.

The sequence that takes place in deriving the scattering matrix in terms of the wave amplitudes is intricate and uses a transformation for the state vector from beam cross sectional properties to traveling waves. In this process, the control function derived is essentially $\sqrt{s}$ based.

$$C(s) = \frac{M_c(s)}{\theta(s)} = \frac{\sqrt{2}(EI)^{\frac{3}{4}}(\rho A)^{\frac{1}{4}}}{3}\sqrt{s} \tag{9}$$

The control law is effectively a "half differentiator". It is similar to velocity feedback with a 45° instead of 90° phase lead. In order to implement this control law, the function $\sqrt{s}$ had to be estimated by a rational transfer function. The function used was:

$$\sqrt{s} = \frac{(s+10^{-4})(s+10^{-2})(s+10^{0})(s+10^{2})}{(s+10^{-3})(s+10^{-1})(s+10^{1})(s+10^{3})} \qquad (10)$$

The s-functions were then transformed to the z-domain (discretized) prior to forming the closed loop system. The relationship between the continuous domain (s) and the discreet domain (z) is:

$$z = e^{sT}$$

where T is the sampling period. The transfer functions were transformed to the discreet domain using a Tustin transformation for the structure and a matched pole-zero technique for the controller. The system was then simulated on the FSS with the following results:

	Frequency	Damping Ratio
Free Response	0.95	0.0039
H_∞ Control	0.98	0.037
Derivative Control	0.96	0.039

Table 2

III. Current Work

The implementation of a MIMO optimal controller using Linear Quadratic Gaussian (LQG) control theory is being analyzed on the FSS. A two actuator, three sensor arrangement is currently being evaluated as a viable control method for flexible spacecraft structures. The experimental setup involves a "L" shaped flexible arm attached to the main body of the FSS. Two nearly collocated sensor/actuator pairs are mounted on the two beams of the arm at each beam's respective root as shown in Figure 17. A Vision Server camera system is mounted overhead the granite table and senses position and rotation information on the tip of the flexible arm. The sensor information is then fed back into the LQG controller which, along with the sensor information from the piezo wafers, minimizes the rotation of the tip.

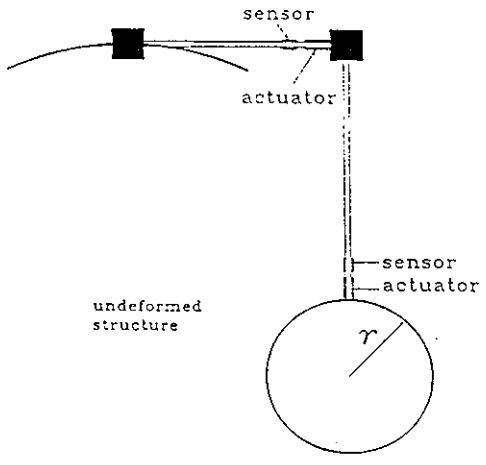

Figure 17. FSS Experimental Setup for LQG/Vision Server Testing

The Vision Server camera system consists of a single infrared CCD camera situated above the test area with Real Time Innovations. Inc. Pointgrabber software interface for the real-time operating system, VxWorks.

Another area of interest is antenna shape control. At this time feasibility studies and literature research is being conducted to evaluate whether piezoceramics can be used for structural shape control, namely in the antenna regime. Normally, antennas use multiple feedhorns to alter their beam pattern, using reflector shape control by using smart structures a single feedhorn can be used for a variety of beam patterns. This research is in the developmental stage and looks promising in the near future.

IV. Future Work

Future work will involve more emphasis on vibration isolation and antenna shape control. Also, application specific experimental work will be the main thrust of the Spacecraft Controls Laboratory Team. New interest in the use of smart structures for vibration reduction of rotorcraft holds some promise with the use of piezoceramic and magnetostrictive actuators. Further analysis into the state-of-the-art actuation devices is to be studied and tested for possible implementation into smart structures

V. Conclusions

The main thrust to date in the Spacecraft Controls Laboratory design team has been to analyze, test and evaluate various control schemes for smart structure technology. Positive Position Feedback has been used extensively in the smart structures area and is a good single mode damping control law. Strain Rate Feedback (SRF) has also been tested and is a good way to get generalized damping for all modes. Classical PID control has been used and compared against PPF and SRF and for certain types of applications and is a suitable control scheme. Wave absorbing H_∞ control has been analyzed and tested and showed good results as a low authority controller. MIMO control using LQG is expected to produce satisfactory results and should fare to be a viable control scheme as well. The NPS Spacecraft Controls Laboratory design team is proactive in its research with state-of-the-art materials and concepts and plans on expanding its capabilities in the near future.

VI. References

(1) Bronowicki, Allen and Betros, Robert, "Design and Implementation of Active Structures", Active Structures Workshop, TRW Space and Electronics Group, Redondo Beach , CA.

(2) Agrawal, B.N., Bang, H., and Jones, E., IAF-92-0319, "Application of Piezoelectric Actuators and Sensors in the Vibration Control of Flexible Spacecraft Structures", 43rd Congress of the International Astronautical Federation, Washington, DC, 1992.

(3) Newman, Scott M., "Active Damping Control of a Flexible Space Structure using Piezoelectric Sensors and Actuators", Master's Thesis, Naval Postgraduate School, December 1992.

(4) Feuerstein, Mark G., "A Comparison of Different Control Methods for Vibration Suppression of Flexible Structures Using Piezoelectric Actuators", Master's Thesis, Naval Postgraduate School, June 1994.

(5) Agrawal, B.N. and Bang, H., IAF-94-I.4.202, "Adaptive Structures for Large Precision Antennas", 45th Congress of the International Astronautical Federation, Jerusalem, Israel, 1994.

(6) Strong, Ronald E., "Control of Flexible Spacecraft Structures using H-Infinity Wave Absorbing Control", Master's Thesis, December 1994.

(7) von Flotow, A.H., "Traveling Wave Control for Large Spacecraft Structures, Journal of guidance", Vol. 9, No. 4, July-August 1986, pp. 462-468.